Sub-100-nm Lithographic Imaging with an EUV 10x Microstepper

John E. M. Goldsmith*[a], Kurt W. Berger[a], Danny R. Bozman[a], Gregory F. Cardinale[a], Daniel R. Folk[a], Craig C. Henderson[a], Donna J. O'Connell[a], Avijit K. Ray-Chaudhuri[a], Kenneth D. Stewart[a], Daniel A. Tichenor[a], Henry N. Chapman[b], Richard Gaughan[b], Russell M. Hudyma[b], Claude Montcalm[b], Eberhard A. Spiller[b], John S. Taylor[b], Jeffrey D. Williams[b], Kenneth. A. Goldberg[c], Eric M. Gullikson[c], Patrick Naulleau[c], and Jonathan L. Cobb[d]

[a]Sandia National Laboratories, MS 9409, PO Box 969, Livermore, CA 94550

[b]Lawrence Livermore National Laboratory, PO Box 808, Livermore, CA 94550

[c]Lawrence Berkeley National Laboratory, Berkeley, CA 94720

[d]Motorola c/o EUV,LLC, Sandia National Laboratories, PO Box 969, Livermore, CA 94550

ABSTRACT

The capabilities of the EUV 10x microstepper have been substantially improved over the past year. The key enhancement was the development of a new projection optics system with reduced wavefront error ($\lambda_{EUV}/20$), reduced flare (<5%), and increased numerical aperture (0.088 round or 0.1x0.088 rectangular, interchangeable). These optics and concomitant developments in EUV reticles and photoresists have enabled dramatic improvements in EUV imaging, illustrated by resolution of 70 nm dense (1:1) lines and spaces (L/S). CD linearity has been demonstrated for dense L/S over the range 200 nm to 80 nm, both for the imaging layer and for subsequent pattern transfer. For a ±10% CD specification, we have demonstrated a process latitude of ±0.8 μm depth of focus and 10% dose range for dense 90 nm L/S, and ±1 μm depth of focus and 10% dose range for dense 100 nm L/S.

Keywords: EUV, extreme ultraviolet, lithography, microlithography, stepper, microstepper

1. INTRODUCTION

The EUV 10x microstepper was described in detail in a previous paper in this conference series.[1] Since that time, the cluster jet laser-produced plasma source (LPS)[2,3] has replaced the copper-wire-based LPS, and it has produced excellent results in the integrated imaging system (Fig. 1). The microstepper has also been used for further sensor development, including a wafer-stage dose sensor and an aerial image monitor. This paper, however, focuses on sub-100-nm imaging studies that have been made possible by new 10x projection optics systems that have been developed during the past year. Two nearly identical projection systems were assembled, one for use in the microstepper, and the second for use in the "10xI" imaging system.[4] During the period that the microstepper was used primarily for jet-source and sensor studies, the majority of the imaging studies (including those described in this paper) were carried out using the 10xI imaging system. In addition to leading to the development of improved EUV photoresists (obtained from commercial suppliers) and refined reticle fabrication techniques, these studies have also led to an improved understanding of the detailed lithographic characteristics of the 10x imaging systems.

* Correspondence: Email jgold@ca.sandia.gov; Telephone 925-294-2432; Fax: 925-294-3870

Part of the SPIE Conference on Emerging Lithographic Technologies III
Santa Clara, California • March 1999
SPIE Vol. 3676 • 0277-786X/99/$10.00

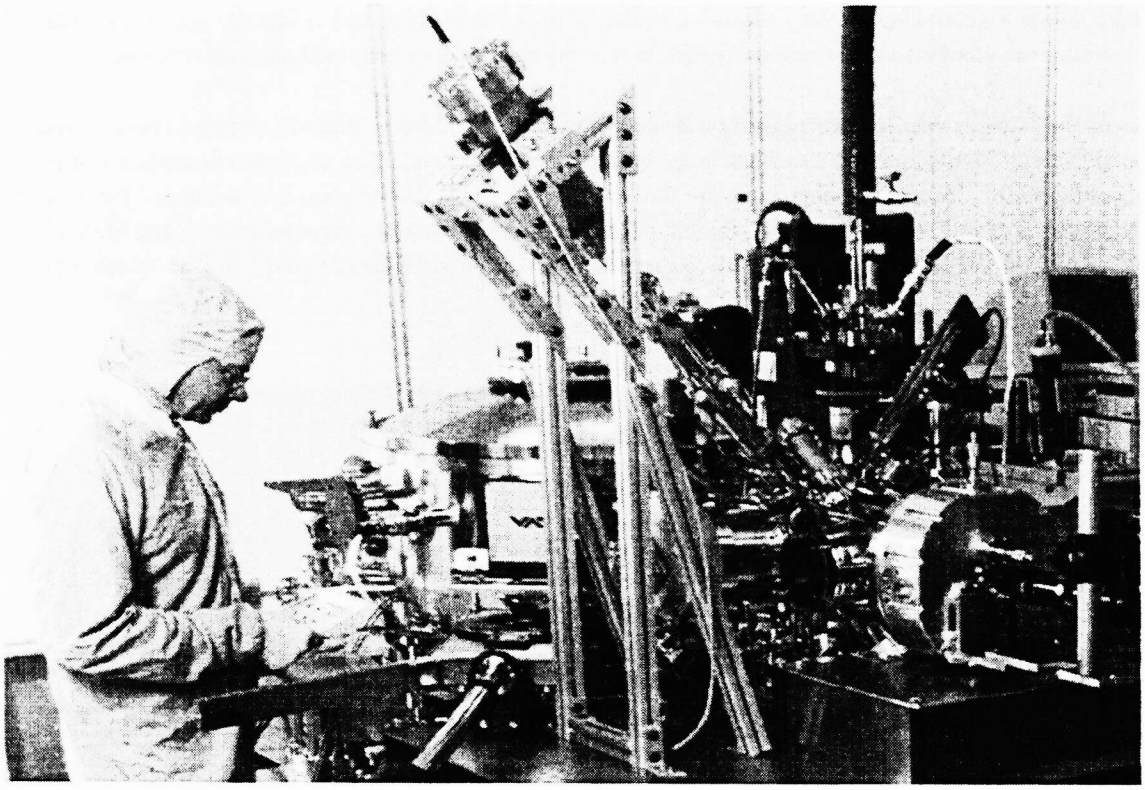

Fig. 1. EUV 10x microstepper with xenon jet laser-produced plasma source

2. PROJECTION OPTICS

The development of improved projection optics systems (or "cameras") has provided the most significant enhancement in the capabilities of the 10x systems. The key advances that led to the improvements were in the areas of substrate manufacture, multilayer coatings, at-wavelength characterization of coated elements and assembled cameras, and alignment techniques that take advantage of advanced visible-wavelength interferometry. During the past year, we have assembled and produced images using two nearly identical 10x cameras that exploit these advances. The cameras are mechanically and optically compatible with both 10x imaging systems, and also with the EUV phase-shifting point diffraction interferometer.[5]

The Schwarzschild camera has spherical surfaces that are 16 mm (convex primary) and 90 mm (concave secondary) in diameter, but only small off-axis subapertures are used for EUV imaging (5 mm and 25 mm, respectively). We take advantage of this characteristic by recording visible-wavelength interferograms of the individual substrates, and then performing computer "clocking" of the simulated camera to select subapertures that provide optimum performance. The substrates were fabricated to specifications[6] very similar to those for the Engineering Test Stand (ETS),[7] an "alpha-class" EUVL imaging tool currently being developed. In addition to the requirement for sub-nm rms figure error needed for diffraction-limited imaging performance, low values of high- and mid-spatial-frequency roughness are crucial for obtaining high reflectivity and low flare (scattered light), respectively.

The relatively large variation of angle of incidence across the camera subaperture requires that the thickness of the Mo/Si multilayer reflective coatings[8] be graded in order to optimally reflect the same wavelength across the subaperture (the multilayer period must increase as a function of distance from the center of the mirror). In order to assure that the coatings will produce no degradation of the imaging performance of the camera, we chose $\Delta\lambda<0.05$ nm as the goal for matching the coatings, corresponding to a maximum fractional variation in multilayer period of 0.4%. In addition to requiring high peak

reflectivity, high *net* throughput also requires careful matching of the center wavelength of the two optical elements (<0.1 nm at the 13.4 nm center wavelength). The coatings applied to these substrates are nearly perfect in all respects.[9]

The alignment of the cameras was performed using a visible-wavelength (532 nm) optical-fiber-based phase-shift diffraction interferometer (PSDI).[10] Figure 2 shows a camera in the interferometer teststand. The alignment procedure was based on measurements of the EUV subaperture using a routine similar to the (much more complex) one developed for the ETS.[11] To verify the methodology of visible-wavelength alignment of EUV cameras, we have compared visible- and EUV-wavelength interferograms of several 10x cameras.[12] The result of these comparisons is confidence that the rms wavefront errors of the two cameras are $\sim\lambda_{EUV}/20$.

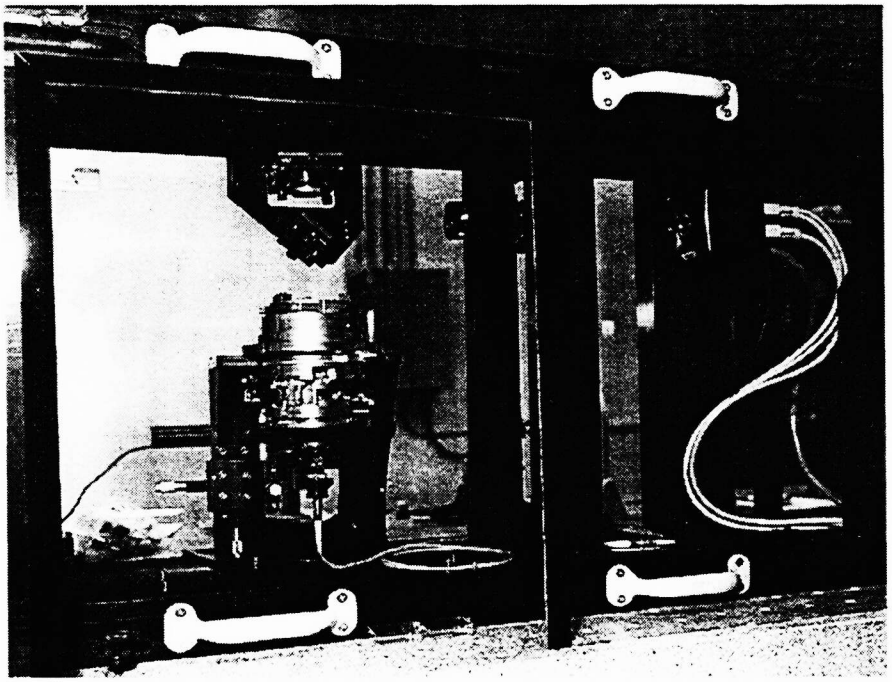

Fig. 2. 10x camera in visible-wavelength interferometer teststand

The characteristics of the substrates and assembled cameras are summarized in Table 1. Characterization of the flare of the cameras is treated in detail in an accompanying paper.[13]

Table 1. Characteristics of new 10x projection optics systems (NA: numerical aperture; WFE, wavefront error). The primary is the smaller, convex mirror, the secondary the larger, concave mirror. Mid-spatial frequency-roughness (MSFR) and high-spatial-frequency roughness (HSFR) correspond to integration of the surface power spectral density over the frequency bands 1 mm^{-1} to 1 μm^{-1} (MSFR) and 1 μm^{-1} to 50 μm^{-1} (HSFR) measured on the uncoated substrates.

Camera	NA	WFE (rms EUV waves)	Primary		Secondary			Flare	
			MSFR (nm)	HSFR (nm)	MSFR (nm)	HSFR (nm)	Reflec-tivity	Calc.	Meas.
1	0.088	0.05	0.17	0.09	0.22	0.16	65.4%	4%	4.5%
2	0.088	0.05	0.13	0.10	0.20	0.19	63.1%	3%	

3. LITHOGRAPHIC RESULTS

The resist images shown in this section illustrate the capabilities of the new 10x cameras. All images shown were recorded in a customized DUV resist exposed in a thin layer (typically 80-100 nm). The characteristics of ultrathin resists for EUV lithography are discussed in an accompanying paper.[14] As illustrated below, we have demonstrated a resolution for 1:1 L/S of 80 nm at NA 0.088 and 70 nm at NA 0.10; with the process "k_1" factor defined by the standard lithographic expression resolution $R = k_1 \times \lambda/NA$, both results yield k_1=0.52. It is worth pointing out that maintaining this process factor with a system designed[15] to support an NA of 0.25 would potentially provide 28-nm resolution.

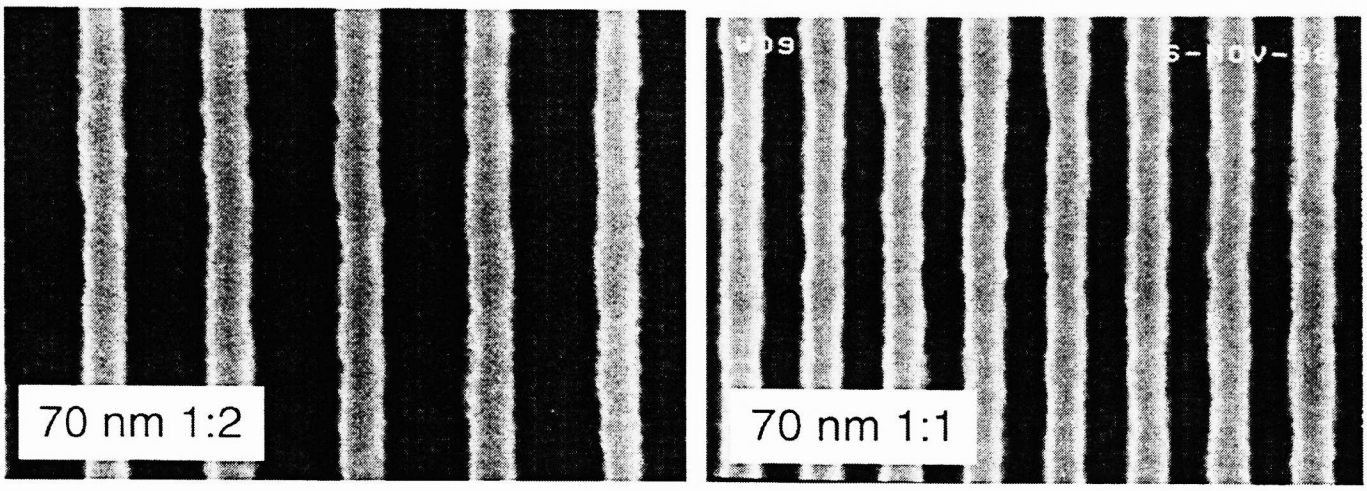

Fig. 3. 70 nm L/S at 1:2 pitch and 1:1 pitch (Camera 1 at NA 0.10).
Measured LER values (3σ one side) are 6.9 nm for the 1:2 L/S and 6.7 nm for the 1:1 L/S.

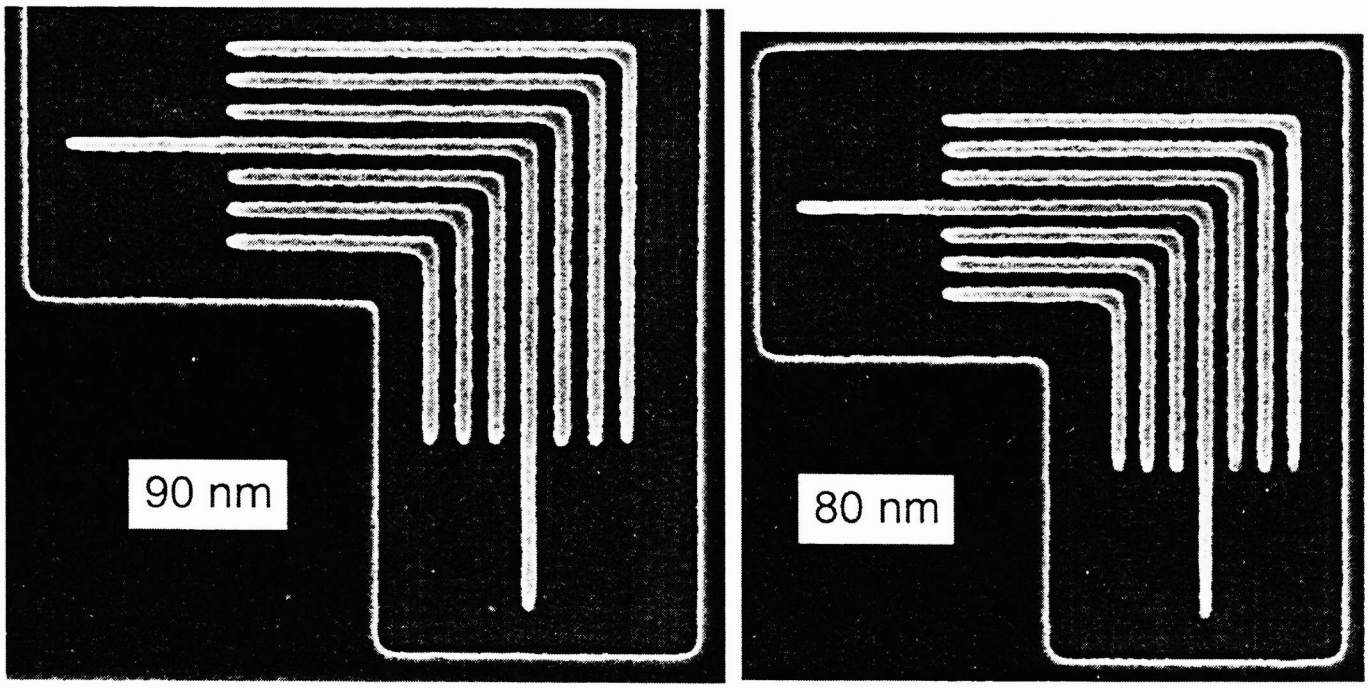

Fig. 4. Iso-dense elbow patterns (Camera 2 at NA 0.088).

We have also begun investigating the effectiveness of a thin layer of DUV resist as an etch stop for pattern transfer into an underlying hard mask. Figure 5 illustrates pattern transfer into a 350-nm thick layer of polySi using an 80-nm thick layer of DUV photoresist with an intermediate 50-60 nm low-temperature oxide (LTO) layer as a hard mask.

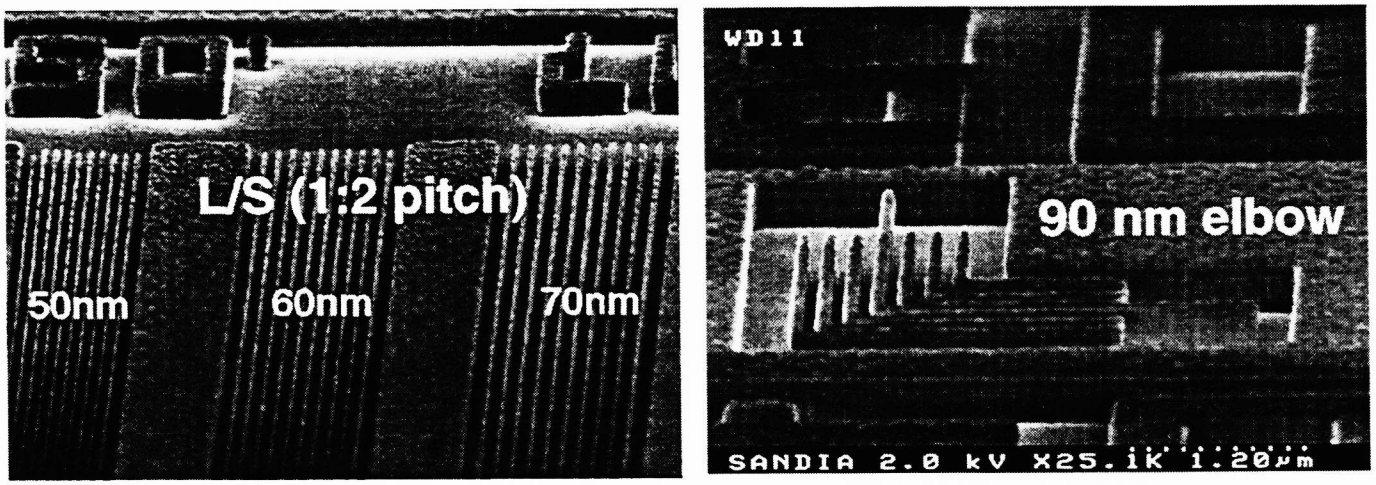

Fig. 5. Sub-100-nm features etched through 350 nm polySi (Camera 1 at NA 0.088).

Figures 6-8 demonstrate linearity and depth-of-focus characterization measurements for the new cameras. Linearity is observed down to approximately 80 nm for dense L/S (Fig. 9). For a ±10% CD specification, Figs. 10 and 11 demonstrate a process latitude of ±0.8 µm depth of focus and 10% dose range for dense 90 nm L/S, and ±1 µm depth of focus and 10% dose range for dense 100 nm L/S.

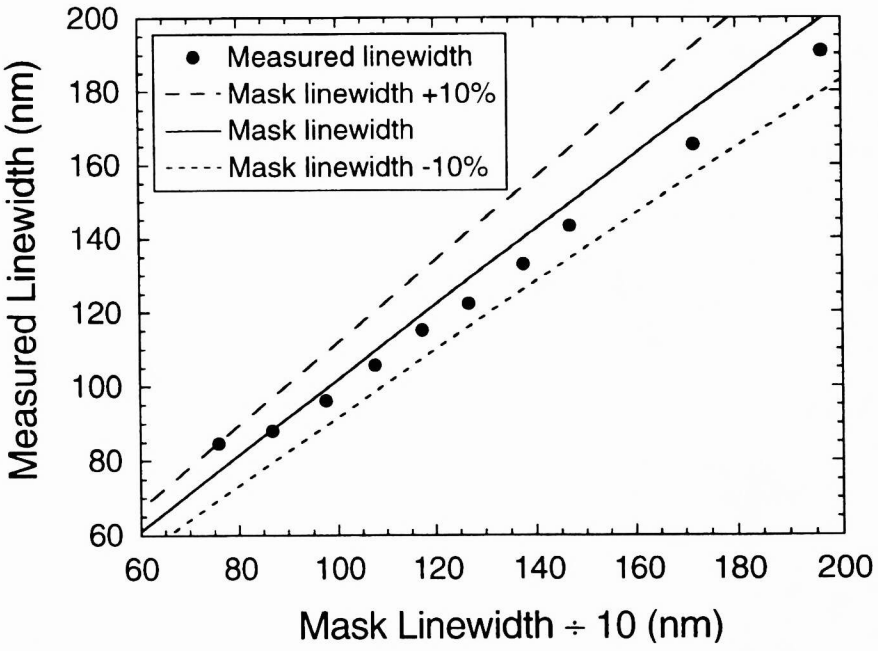

Fig. 6. Linearity characterization for dense L/S with pattern transfer (after etch through 350 nm polySi, Camera 1 at NA 0.088).

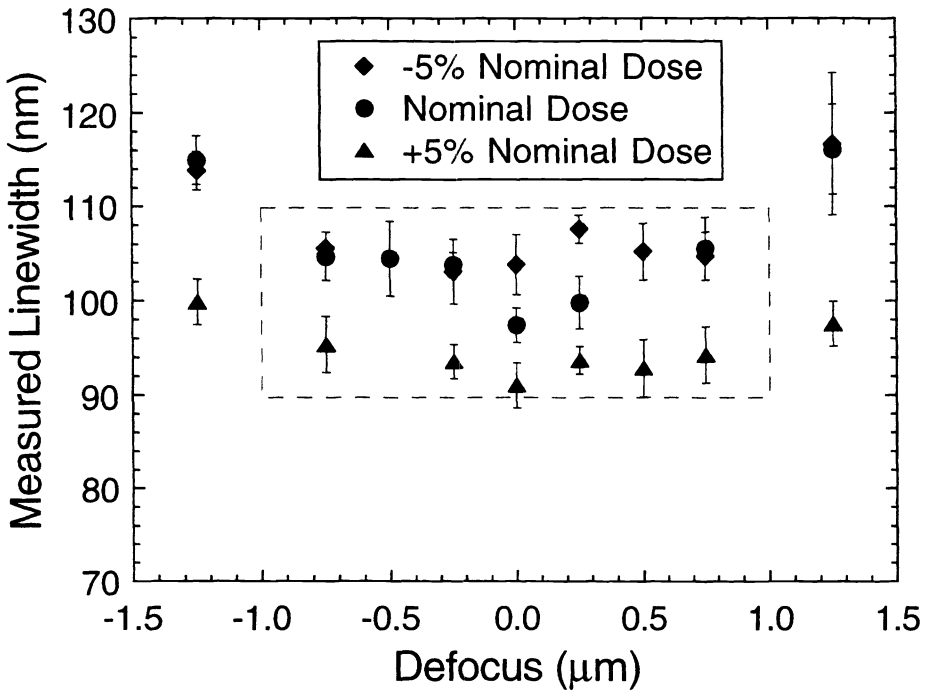

Fig. 7. Process latitude of camera 2 at NA 0.088 for 100 nm dense L/S with a ±10% CD specification.

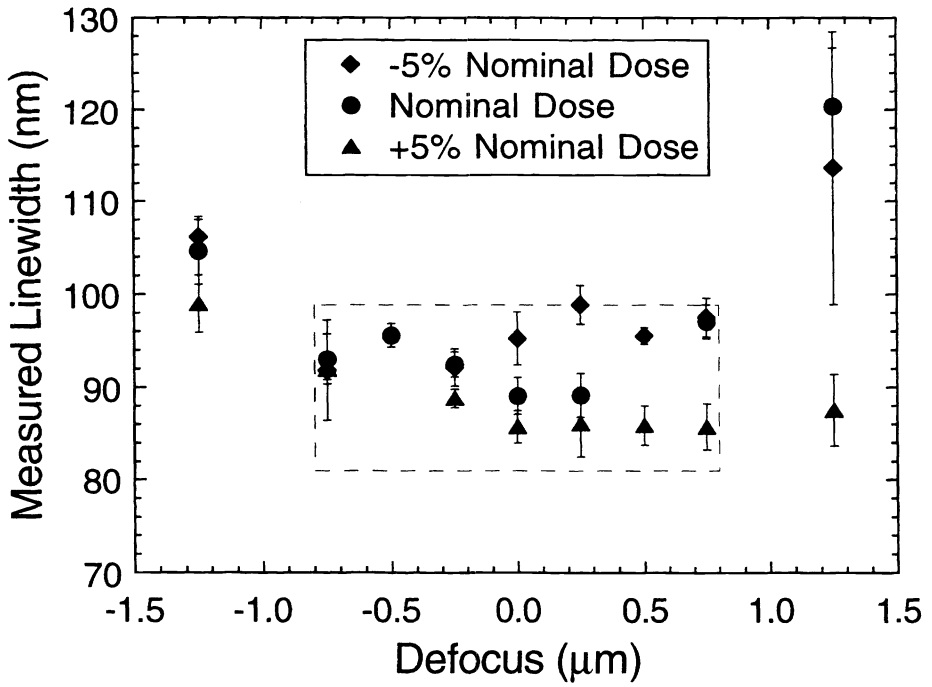

Fig. 8. Process latitude of camera 2 at NA 0.088 for 90 nm dense L/S with a ±10% CD specification.

4. CONCLUSION

Several important research areas that depend on the capabilities of the 10x imaging systems have not been described here, including sensor development, and imaging studies of programmed phase and amplitude defects. Nonetheless, the lithographic results that are presented in this paper demonstrate the advances in EUV imaging made possible by the development of improved projection optics systems (wavefront error ~$\lambda_{EUV}/20$, flare <5%), photoresists, and reticles. In particular, we have demonstrated CD linearity for dense L/S features as small as 80 nm, and a depth of focus of nearly ±1 μm for 90 nm dense L/S. Finally, imaging of 80 nm iso-dense elbow patterns with an NA of 0.088, and 70 nm dense L/S with an NA of 0.10, both support extendibility of EUV to the 30 nm node through a reasonable increase in numerical aperture.

ACKNOWLEDGEMENTS

This work was performed under the auspices of the U. S. Department of Energy by Sandia National Laboratories under contract DE-AC04-94AL85000, by Lawrence Livermore National Laboratory under Contract No. W-7405-ENG-48, and by Lawrence Berkeley National Laboratory. Funding was provided by the Extreme Ultraviolet Limited Liability Company (EUV LLC) under a Cooperative Research and Development Agreement and by I-SEMATECH.

REFERENCES

1. J. E. M. Goldsmith, P. K. Barr, K. W. Berger, L. J. Bernardez II, G. F. Cardinale, J. R. Darnold, D. R. Folk, S. J. Haney, C. C. Henderson, K. L. Jefferson, K. D. Krenz, G. D. Kubiak, R. P. Nissen, D. J. O'Connell, Y. E. Perras, A. K. Ray-Chaudhuri, T. G. Smith, R. H. Stulen, D. A Tichenor, A. A. Ver Berkmoes, and J. B. Wronosky, "Recent advances in the Sandia EUV 10x microstepper," in *Emerging Lithographic Technologies II*, Yuli Vladimirsky, Editor, Proc. SPIE 3331, pp. 11-19 (1998).

2. G. D. Kubiak, L. J. Bernardez, K. D. Krenz, D. J. O'Connell, R. Gutowski, and A. M. M. Todd, "Debris-free EUVL sources based on gas jets," in *OSA Trends in Optics and Photonics Vol. 4, Extreme Ultraviolet Lithography*, G. D. Kubiak and D. Kania, Editors, pp. 66-71 (Optical Society of America, Washington, DC, 1996).

3. G. D. Kubiak, L. J. Bernardez, and K. D. Krenz, "High-power extreme ultraviolet source based on gas jets," in *Emerging Lithographic Technologies II*, Yuli Vladimirsky, Editor, Proc. SPIE 3331, pp. 81-89 (1998).

4. D. A. Tichenor, G. D. Kubiak, M. E. Malinowski, R. H. Stulen, S. J. Haney, K. W. Berger, R. P. Nissen, R. L. Schmitt, G. A. Wilkerson, L. A. Brown, P. A. Spence, P. S. Jin, W. C. Sweatt, W. W. Chow, J. E. Bjorkholm, R. R. Freeman, M. D. Himel, A. A. MacDowell, D. M. Tennant, O. R. Wood, II, W. K. Waskiewicz, D. L. White, D. L. Windt and T. E. Jewell, "Development and characterization of a 10× Schwarzschild system for soft-x-ray projection lithography," *OSA Proceedings on Soft X-Ray Projection Lithography*, A. M. Hawryluk and R. H. Stulen, Editors, Vol. 18, pp. 79-82 (Optical Society of America, Washington, DC, 1993).

5. P. Naulleau, K. A. Goldberg, E. Tejnil, S. H. Lee, H. Medicki, C. J. Bresloff, P. J. Batson, P. Denham, D. T. Attwood, Jr., and J. Bokor, "Characterization of the accuracy of EUV point diffraction interferometry," in *Emerging Lithographic Technologies II*, Yuli Vladimirsky, Editor, Proc. SPIE 3331, pp. 114-123 (1998).

6. J. S. Taylor, G. E. Sommargren, D. W. Sweeney, and R. M. Hudyma, "The fabrication and testing of optics for EUV projection lithography," in *Emerging Lithographic Technologies II*, Yuli Vladimirsky, Editor, Proc. SPIE 3331, pp. 580-590 (1998).

7. D. W. Sweeney, R. Hudyma, H. N. Chapman, and D. Shafer, "EUV optical design for a 100 nm CD imaging system," in *Emerging Lithographic Technologies II*, Yuli Vladimirsky, Editor, Proc. SPIE 3331, pp. 2-10 (1998).

8. C. Montcalm, S. Bajt, P. B. Mirkarimi, E. Spiller, F. J. Weber, and J. A. Folta, "Multilayer reflective coatings for extreme-ultraviolet lithography," in *Emerging Lithographic Technologies II*, Yuli Vladimirsky, Editor, Proc. SPIE 3331, pp. 42-51 (1998).

9. C. Montcalm, E. Spiller, M. Wedowski, E. M. Gullikson, and J. A. Folta, "Multilayer coatings of 10x projection optics for extreme-ultraviolet lithography," in *Emerging Lithographic Technologies III*, Y. Vladimirsky, Editor, Proc. SPIE 3676, this volume (1999).

10. G. E. Sommargren, "Phase shifting diffraction interferometry for measuring extreme ultraviolet optics," in *OSA Trends in Optics and Photonics Vol. 4, Extreme Ultraviolet Lithography*, G. D. Kubiak and D. Kania, Editors, pp. 108-112 (Optical Society of America, Washington, DC, 1996).

11. H. N. Chapman and D. W. Sweeney, "A rigorous method for compensation selection and alignment of microlithographic optical systems," in *Emerging Lithographic Technologies II*, Yuli Vladimirsky, Editor, Proc. SPIE 3331, pp. 102-113 (1998).

12. K. A. Goldberg, P. Naulleau, R. Gaughan, H. Chapman, J. E. M. Goldsmith, and J. Bokor, "Direct comparison of EUV and visible-light interferometries," in *Emerging Lithographic Technologies III*, Y. Vladimirsky, Editor, Proc. SPIE 3676, this volume (1999).

13. E. M. Gullikson, P. Naulleau, K. A. Goldberg, S. Baker, C. Montcalm, E. Spiller, J. S. Taylor, J. Bjorkholm, D. G. Stearns, and J. E. M. Goldsmith, "The characterization of flare for EUV 10x projection cameras," in *Emerging Lithographic Technologies III*, Y. Vladimirsky, Editor, Proc. SPIE 3676, this volume (1999).

14. V. Rao, J. L. Cobb, C. C. Henderson, U. Okoroanyanwu, D. R. Bozman, P. Mangat, R. L. Brainerd, and J. Mackevich, "Ultrathin photoresists for extreme ultraviolet lithography," in *Emerging Lithographic Technologies III*, Y. Vladimirsky, Editor, Proc. SPIE 3676, this volume (1999).

15. R. M. Hudyma and D. R. Shafer, "Design of high numerical aperture designs for EUV projection lithography," in *Emerging Lithographic Technologies III*, Y. Vladimirsky, Editor, Proc. SPIE 3676, this volume (1999).